AD-A078 684 MICHIGAN UNIV ANN ARBOR COLL OF ENGINEERING F/G 20/9
THEORETICAL STUDIES OF LASER LIGHT INTERACTION AND OPTICAL AND --ETC(U)
NOV 79 J J DUDERSTADT , R S ONG AFOSR-76-2904
UNCLASSIFIED AFOSR-TR-79-1303 NL

1 OF 1
AD
A078684

END
DATE
FILMED
1-80
DDC

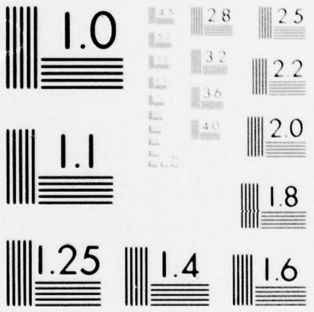
1.0
1.1
1.25
1.4
1.6
1.8
2.0
2.2
2.5
2.8
3.2
3.6
4.0
4.5
5.0

MICROCOPY RESOLUTION TEST CHART
NATIONAL BUREAU OF STANDARDS-1963-A

AFOSR-TR- 79-1303

LEVEL II

(12)

ADA078684

Final Report

Theoretical Studies of Laser Light Interaction and Optical and X-Ray Emission from Dense Metallic Plasmas

J.J. DUDERSTADT
R.S.B. ONG

DDC
DEC 18 1979
RECEIVED
E

November 1979

DDC FILE COPY

United States Air Force
Office of Scientific Research
Grant No. AFOSR 76-2904

THE UNIVERSITY OF MICHIGAN 1817
College of Engineering
Departments of Aerospace and Nuclear Engineering

Approved for public release;
distribution unlimited.

79 12 18 28

UNCLASSIFIED
SECURITY CLASSIFICATION OF THIS PAGE (When Data Entered)

(19) REPORT DOCUMENTATION PAGE

READ INSTRUCTIONS
BEFORE COMPLETING FORM

1. REPORT NUMBER
(18) AFOSR-TR-79-1303

2. GOVT ACCESSION NO.

3. RECIPIENT'S CATALOG NUMBER

4. TITLE (and Subtitle)
(6) Theoretical Studies of Laser Light Interaction and Optical and X-ray Emission from Dense Metallic Plasmas.

5. TYPE OF REPORT & PERIOD COVERED
(9) Final Rep~~or~~t. 1 Aug 75 - 1 Oct 79

6. PERFORMING ORG. REPORT NUMBER

7. AUTHOR(s)
(10) J.J. Duderstadt ~~and~~ R.S.B. Ong

8. CONTRACT OR GRANT NUMBER(s)
(15) ✓AFOSR-76-2904 new

9. PERFORMING ORGANIZATION NAME AND ADDRESS
The University of Michigan
Ann Arbor, MI 48109

10. PROGRAM ELEMENT, PROJECT, TASK AREA & WORK UNIT NUMBERS
(17) A2
(16) 2301/A2 61102F

11. CONTROLLING OFFICE NAME AND ADDRESS
Air Force Office of Scientific Research/NP
Bldg. 410, Bolling AFB, D.C. 20332

12. REPORT DATE
(11) Nov~~ember~~ 1979

13. NUMBER OF PAGES
50

14. MONITORING AGENCY NAME & ADDRESS (if different from Controlling Office)
(12) 54

15. SECURITY CLASS. (of this report)
Unclassified

15a. DECLASSIFICATION/DOWNGRADING SCHEDULE

16. DISTRIBUTION STATEMENT (of this Report)

Approved for public release;
distribution unlimited.

17. DISTRIBUTION STATEMENT (of the abstract entered in Block 20, if different from Report)

18. SUPPLEMENTARY NOTES

19. KEY WORDS (Continue on reverse side if necessary and identify by block number)
Laser-Plasma Interaction Exploded Wire, X-ray Emission, Stimulated Brillouin Scattering, Thermal Self-Focusing, Resonance Absorption, Wave-Breaking, Radiation Transport Processes

79 12 18 28

20. ABSTRACT (Continue on reverse side if necessary and identify by block number)
The interaction of a high power CO_2 laser with a dense plasma is investigated. Stimulated Brillouin scattering and thermal self-focusing of the incident beam is studied. The dynamics of a strongly turbulent plasma generated by laser-plasma interaction, and the behavior of nonlinear waves (solitons) in the plasma is analyzed. Advanced MHD plasma simulation models are employed to study the complex dynamics of nonequilibrium plasmas interacting with laser radiation. MHD computer codes capable of simulating exploding wire or pinch dynamics subjected to intense laser irradiation are developed. Radiation transport effects, such as → over

DD FORM 1 JAN 73 1473 228 650 UNCLASSIFIED

X-ray line emission and re-absorption in optically thick regions of the plasma, are incorporated in the MHD computer code.

12

THEORETICAL STUDIES OF LASER LIGHT INTERACTION AND OPTICAL AND X-RAY EMISSION FROM DENSE, METALLIC PLASMAS

FINAL REPORT

J.J. Duderstadt
R.S.B. Ong

November 1979

AIR FORCE OFFICE OF SCIENTIFIC RESEARCH (AFSC)
NOTICE OF TRANSMITTAL TO DDC
This technical report has been reviewed and is
approved for public release IAW AFR 190-12 (7b).
Distribution is unlimited.
A. D. BLOSE
Technical Information Officer

United States Air Force
Office of Scientific Research
Grant No. AFOSR 76-2904

Accession For
NTIS GRA&I ☑
DDC TAB ☐
Unannounced ☐
Justification
By
Distribution/
Availability Codes
Dist A
Avail and/or special

College of Engineering
Departments of
Aerospace and Nuclear Engineering

This final report describes the achievements of the AFOSR sponsored research program on laser interaction with dense metallic plasmas under Grant AFOSR-76-2904 during the period 1 August, 1975 to 1 October 1979. The principal aim of the research effort is to study the dynamics of a high density, low temperature (10 eV) plasma when illuminated by a high intensity laser beam. The investigation is carried out both theoretically and by means of an advanced numerical simulation code. The following sections give a description of the various efforts and accomplishments. A more detailed description of much of the work may be found in our three Annual Reports (1976, 1977, and 1978) and the several Progress Reports submitted earlier. The first few sections cover the theoretical effort followed by a description of the numerical simulation code investigation.

A. STIMULATED BRILLOUIN SCATTERING IN A HIGH-DENSITY Z-PINCH AND EXPLODED WIRE PLASMAS

An important part of the research program concerns stimulated Brillouin scattering (SBS) in magnetized plasmas. Most important effects are included in our investigation, such as magnetic fields, plasma temperature, arbitrary angle of propagation of the stimulated waves, boundedness of the plasma, and density inhomogeneities. The dispersion relation describing the stimulated Brillouin scattering was derived and analyzed.

The inclusion of a background magnetic field has led to several new results. A magnetosonic mode of the plasma is found to be driven across field lines instead of the usual ion acoustic wave in the magnetic field free case. Because the damping rate of the high frequency Alfvén wave is lower than the damping rate of the ion acoustic wave ($T_e \simeq T_i$) the threshold of the instability is correspondingly lowered. The addition of the magnetic field inhomogeneity causes a larger wave vector mismatch than in the field free case. This inhibits growth of SBS in nonuniform plasmas because the waves convect more quickly out of the unstable region (see D.J. Kenney and R.S.B. Ong, Technical Report, August 1976).

B. FINITE AMPLITUDE WAVES IN A MAGNETIZED PLASMA

The interaction of an intense laser beam with a magnetized plasma generates density and electric field fluctuations in the plasma via the saturation of various instabilities. Thus finite amplitude waves are present in the disturbed plasma. Therefore it is important to study the nonlinear behavior of these finite amplitude waves. In this respect we solved the problem of the long time behavior of a monochromatic finite amplitude shear Alfvén wave. It is shown that the nonlinear coupling between the Alfvén pump wave and a background sound wave in the plasma gives rise to forced magnetic sidebands. The Alfvén pump wave as well as the sidebands steepen up in the long time scale. This is shown by applying a stability analysis to the nonlinear Schrödinger equation derived for these nonlinear finite amplitude waves (see J. Ionson and R.S.B. Ong, Technical Report, October 1975).

C. DYNAMICS OF THE IRRADIATED PLASMA; PONDEROMOTIVE FORCE AND SOLITON GENERATION

We consider a large amplitude electromagnetic wave incident on the critical surface (where the electron plasma frequency equals the incident wave frequency) of a dense plasma; the ponderomotive force generated acts to expell matter from the region of high field intensity forming a density depression. This depression serves to trap the electric field, enhancing the ponderomotive force, which in turn deepens the cavity. In this manner the trapped electric is able to reach a very large amplitude. Its envelope has the shape of a solitary wave and is described by a Schrödinger equation with a nonlinear potential. The nonlinearity in the potential is of the exponential type; it shows an exponential decrease as the electric field increases. In many treatments of the problem the exponential term is usually expanded and higher order terms in the series expansion are then neglected. The consequence of such a truncation is that the density becomes unphysical as the electric field grows instead of decreasing. On the other hand the inclusion of the exponential forces the field to saturate at large values in agreement with observation.

We have retained the exponential form of the potential in the nonlinear Schrödinger equation and solved for the envelope numerically. The result is a solitary pulse or "soliton". We also showed that the soliton solution is a singular solution of the nonlinear Schrödinger equation possessing an exponential nonlinearity.

D. THERMAL SELF-FOCUSING OF LASER LIGHT IN A DENSE PLASMA

The problem investigated in this part of the research arises from experimental results observed by the experimental group in our laboratory. A CO_2 laser is directed perpendicularly to an over-dense plasma column, and the transitted intensity of the beam is measured as a function of the incident power level. Two results have been observed: first, the transmitted intensity shows a threshold effect as a function of the incident power. As the incident power is increased, the transmitted intensity jumps discontinuously. Below a certain laser intensity no transmission is observed. Second, when a photographic plate is placed to observe the transmitted light, a Fresnel diffraction pattern is recorded. This pattern suggests that the transmitted beam emerges from a sharp hole in the over-dense plasma.

In order to explain the above results we make use of the theory of thermal self-focusing of a laser beam in a plasma. As the laser beam interacts with the plasma the large amplitude oscillating electric field of the beam couples to the electrons in the plasma. The frequency of the oscillating wave electric field is too high for the massive ions to follow. The process transfers electric field energy to kinetic energy in the electrons. The net effect is an increase in the electron temperature inside the beam area. The energy of the electrons acquired from the incident laser beam is calculated as a function of the laser intensity. From the plasma parameters in our laboratory experiment (cf. Annual Report III) we determine that the main energy dissipation mechanism is electron heat conduction in the direction transverse to the axis of the incident laser beam.

Next the electron density distribution in the transverse direction is calculated from the steady state energy balance equation. From the value of the sound speed in our plasma laboratory we determine that the characteristic time scale for hydrodynamic motions transverse to the beam is larger than the temperature equilibration time. Thus we may neglect hydrodynamic motions in the transverse direction. This implies that the electron pressure is approximately constant across the laser beam. As a result the transverse electron density is inversely proportional to the electron temperature distribution. Thus, for an incident laser beam with an electric field having a Gaussian profile the electron heating is nonuniform in the transverse direction. This means that the electron temperature is maximum on the beam axis and decreases in the direction perpendicular to the axis. Consequently the electron density is minimum on the axis of the incident laser beam. This depression in the electron density increases the dielectric constant (and also the index of refraction) of the plasma. It is larger inside the beam than outside. Since light rays bend towards regions of higher dielectric constant, the beam focusses in towards the centerline area. This causes a further increase in the field intensity in the region near the beam axis with a corresponding increase in the value of the dielectric constant of the plasma. This is the process of thermal self-focusing and it enables the laser beam to tunnel itself through an over-dense plasma.

We have mathematically analyzed the thermal self-focusing of the laser beam in our laboratory experiment. The threshold is determined and the laser amplitude profile calculated as it propagates through the plasma (see A. Schmutt and R.S. B. Ong, Technical Report, February 1979).

E. DYNAMICS OF THE STRONGLY TURBULENT PLASMA GENERATED BY LASER-PLASMA INTERACTIONS

A high intensity laser beam disturbs a plasma very violently such that spatially localized electric fields (solitons) may appear. These localized intense fields are basic in the understanding of strongly turbulent plasmas. Further, such localized nonlinear entities can interact strongly with individual electrons and ions thus leading to a significant modification of the zero-order properties of the plasma itself (e.g. density, temperature, flow velocity, etc.).

It is recognized that these localized intense fields (solitons) in unmagnetized plasmas are subject to a collapsing type of instability in more than one dimension. Of course in a real plasma various mechanisms will intervene to prevent total collapse. In particular, if the nonlinear term is the full exponential one, the soliton is stable against collapse. However, this condition implies that the plasmon energy density is of the order of the thermal energy density. But it is well known that such high levels of turbulence are not attainable in plasmas since various mechanisms, such as nonlinear Landau damping, intervene to transfer energy from the waves to the random particle motions.

The presence of a large background magnetic field can improve the situation. It is with this regard that we investigate whether a large background magnetic field could provide the rigidity which would prevent the collapse of solitary waves.

We consider finite amplitude solitary Alfvén wave in a collisionless plasma with a large, externally applied magnetic field. Recent studies showed that in the absence of density perturbations (i.e., the incompressible MHD case) nonlinear Alfvén waves form an axially symmetric waveguide along the ambient magnetic field. The Alfvén wave exhibits a vortex-like behavior inside the waveguide. These results were obtained by retaining second order nonlinear terms in the MHD equations describing Alfvén waves in cylindrical geometry. In addition, exact solitary Alfvén wave solutions of arbitrary amplitudes in two-dimensional plane geometry are obtained by Hasegawa and Mima based on kinetic theory. In their work corrections to all orders in the amplitude consistent with the low $\beta \equiv nT_e/(B_o^2/8\pi)$ approximations are taken into account. The nonlinear wave is shown to have a long structure along the ambient field line. Furthermore, transverse dispersion and nonlinearity give rise to a localization in the perpendicular direction with a characteristic length of an ion Larmor radius. In this paper we present a nonlinear kinetic Alfvén wave structure with axial symmetry about the line of force of the background magnetic field. The full nonlinearity due to the coupling of the density with the longitudinal electric potential is taken into account to all orders in amplitude consistent with the low β approximation.

We assume a low β plasma with a constant background magnetic field in the z-direction. The low β assumption enables us to use the two potential fields ϕ and ψ to describe the electric field, $E_z = -\partial\psi/\partial z$ and $\underset{\sim}{\mathbf{E}} = -\nabla\phi = -\hat{r}\partial\phi/\partial r$, where we have assumed axial symmetry $(\partial/\partial\theta = 0)$. These fields produce only shear perturbations in the magnetic field. Hence we have $B_z = B_o$ = constant, $B_r = 0$, and

$$\frac{\partial B_\theta}{\partial t} = c\left[\frac{\partial E_z}{\partial r} - \frac{\partial E_r}{\partial z}\right] = c\,\frac{\partial^2}{\partial r\partial z}(\phi - \psi) \qquad (1)$$

where E_r is the radial electric field.

Ampère's law yields the following relations:

$$\frac{\partial B_\theta}{\partial z} = -\frac{4\pi}{c} j_r \tag{2}$$

$$\frac{1}{r}\frac{\partial}{\partial r}(rB_\theta) = \frac{4\pi}{c} j_z \tag{3}$$

Because of the low β assumption the dominant contribution to the longitudinal current is made by the electrons. Hence we may write

$$\frac{\partial j_z}{\partial z} = \frac{\partial (e\, n_e)}{\partial t} \tag{4}$$

The low frequency characteristic of the Alfvén wave motion enables the electrons to thermalize along the magnetic field lines. Thus the electron density couples to the longitudinal electric potential ψ via the Boltzmann distribution

$$n_e = n_o \exp(e\psi/T_e) \tag{5}$$

The following transformations are now introduced in order to make the system of Eqs. (1)-(5) dimensionless:

$$\rho \equiv r\Omega/c_s \quad , \quad c_s \equiv \sqrt{T_e/m_i} \quad , \quad \Omega = e\, B_o/m_i c \quad ;$$

$$\tilde{z} = z(\omega_{pi}/c) = z(\omega/V_A) \quad ; \quad \omega_{pi} = (4\pi n_o e^2/m_i)^{\frac{1}{2}} \quad ;$$

$$T \equiv \Omega t \quad ; \quad \tilde{\psi} \equiv e\psi/T_e \quad ; \quad \tilde{\phi} \equiv e\phi/T_e \quad ; \quad \tilde{n} \equiv n_e/n_o \quad ;$$

$$\tilde{E}_z = E_z ec/\omega_{pi} T_e \quad ; \quad \tilde{E}_r = E_r e\, c_s/\Omega\, T_e \quad ; \quad \tilde{B}_\theta \equiv B_\theta/(4\pi n_o T_e)^{\frac{1}{2}} ,$$

where n_o is the unperturbed plasma density. Equation (1) becomes

$$\frac{\partial \tilde{B}_\theta}{\partial T} = \frac{\partial \tilde{E}_z}{\partial \rho} - \frac{\partial \tilde{E}_r}{\partial \tilde{z}} = \frac{\partial^2}{\partial \rho\, \partial \tilde{z}}(\tilde{\phi} - \tilde{\psi}) \tag{6}$$

Combination of Eqs. (3) and (4) yields

$$\rho^{-1}\frac{\partial}{\partial \rho}\left(\rho\,\frac{\partial \tilde{B}_\theta}{\partial \tilde{z}}\right) = \frac{\partial \tilde{n}}{\partial T} \tag{7}$$

In the low β approximation the electrons are tightly bound to the magnetic field lines. Also the longitudinal ion current may be neglected. The ion current is primarily due to the polarization drift in the radial direction. This is obtained by considering the ion guiding center acted upon by an oscillating electric field perpendicular to the background magnetic field. For low frequencies ($\omega \ll \Omega$) the ion equation of motion yields an expression for the ion polarization drift

$$v_r = (e/m_i \, \Omega^2) \, \frac{\partial E_r}{\partial t}$$

where v_r is the ion velocity in the radial direction and E_r is the radial electric field.

Substituting this into Eq. (2) we obtain, in dimensionless units,

$$\frac{\partial \tilde{B}_\theta}{\partial \tilde{z}} = - \tilde{n} \, \frac{\partial \tilde{E}_r}{\partial T} \qquad (8)$$

Equation (8) shows the coupling of the B_θ-field to the transverse electric field via the ion polarization drift.

If we choose a coordinate axis $\xi \cong K_z \, \tilde{z} - T$ moving along z, and scale ρ to K_z, i.e., $\rho = K_z \bar{\rho}$, where $K_z = k_z \, c\Omega/\omega \, \omega_{pi} = V_A/(\omega/k_z)$, we may integrate Eq. (7) and obtain

$$\tilde{n} = 1 - \bar{\rho}^{-1} \frac{\partial}{\partial \bar{\rho}} (\bar{\rho} \, \tilde{B}_\theta) \qquad (9)$$

We rewrite Eq. (6) as

$$- \frac{\partial \tilde{B}_\partial}{\partial \xi} = \frac{\partial \tilde{E}_z}{\partial \rho} - K_z \frac{\partial \tilde{E}_r}{\partial \xi}$$

and Eq. (8) as

$$K_z \frac{\partial \tilde{B}_\theta}{\partial \xi} = \tilde{n} \, \frac{\partial \tilde{E}_r}{\partial \xi}$$

Eliminating $(\partial\tilde{E}_r/\partial\xi)$, we obtain

$$(K_z^{\,2} - \tilde{n})\,\frac{\partial\tilde{B}_\theta}{\partial\xi} = \tilde{n}\,\frac{\partial\tilde{E}_z}{\partial\rho}$$

With the aid of Eq. (5) we may write

$$\tilde{E}_z = -\,\tilde{n}^{-1}\,K_z\,\frac{\partial\tilde{n}}{\partial\xi}$$

Now, eliminating $\tilde{E}_z$ between the last two equations results, after a little manipulation, in the following relation

$$(K_z^{\,2} - \tilde{n})\,\frac{\partial\tilde{B}_\theta}{\partial\xi} = -\,K_z\,\frac{\partial}{\partial\rho}\,\frac{\partial\tilde{n}}{\partial\xi} + \tilde{n}^{-1}\,K_z\,\frac{\partial\tilde{n}}{\partial\xi}\,\frac{\partial\tilde{n}}{\partial\rho}$$

We now use Eq. (9), and define the operator

$$\nabla^2 \equiv \bar{\rho}^{-1}\,\frac{\partial}{\partial\bar{\rho}}\left(\bar{\rho}\,\frac{\partial}{\partial\bar{\rho}}\right)$$

such that, e.g.,

$$\frac{\partial}{\partial\bar{\rho}}\left[\bar{\rho}^{-1}\,\frac{\partial}{\partial\bar{\rho}}\,(\bar{\rho}\tilde{B}_\theta)\right] = \left(\nabla^2 - \frac{1}{\bar{\rho}^2}\right)\tilde{B}_\theta$$

We apply these notations to our equation for $(\partial\tilde{B}_\theta/\partial\xi)$ above and obtain, after some calculations, the following nonlinear wave equation in $\tilde{B}_\theta$:

$$\tilde{n}(K_z^{\,2} - \tilde{n})\,\frac{\partial\tilde{B}_\theta}{\partial\xi} = \tilde{n}\left(\nabla^2 - \frac{1}{\bar{\rho}^2}\right)\frac{\partial\tilde{B}_\theta}{\partial\xi} + \left[\bar{\rho}^{-1}\,\frac{\partial}{\partial\bar{\rho}}\left(\bar{\rho}\,\frac{\partial\tilde{B}_\theta}{\partial\xi}\right)\right]\left(\nabla^2 - \frac{1}{\bar{\rho}^2}\right)\tilde{B}_\theta \qquad (10)$$

Let us assume $\tilde{B}_\theta$ to be harmonic in ξ, i.e. $\tilde{B}_\theta = f(\kappa\bar{\rho})\,\exp\,(i\kappa\xi)$, where $\kappa^2 = K_z^{\,2} - 1$. Making use of Eq. (9), the wave equation, (10), then becomes

$$\left(\nabla^2 - \frac{1}{\bar{\rho}^2}\right)\tilde{B}_\theta - \tilde{n}\,(K_z^{\,2} - \tilde{n})\,\tilde{B}_\theta = 0$$

Define $F \equiv 1 - \tilde{n}$. Then using $K_z^{\,2} = 1 + \kappa^2$, we can write the last equation as

$$\left(\nabla^2 - \frac{1}{\bar{\rho}^2}\right)\tilde{B}_\theta - (1 - F)(\kappa^2 + F)\,\tilde{B}_\theta = 0$$

or

$$\frac{\partial}{\partial\bar{\rho}}\left[\bar{\rho}^{-1}\,\frac{\partial}{\partial\bar{\rho}}\,(\bar{\rho}\tilde{B}_\theta)\right] + \left[F^2 - (1 - \kappa^2)\,F - \kappa\right]\tilde{B}_\theta = 0 \qquad (11)$$

Away from the ambient magnetic field line, i.e., when $\bar{\rho}$ is large, the solution of Eq. (11) may be approximated by a modified Bessel function $K_1(\kappa\bar{\rho})$. Close to the magnetic field line, $\bar{\rho} << 1$, the near field solution is approximated by $I_1(\kappa\bar{\rho})$. Connecting these near and far field approximations, in the region where $\bar{\rho} \sim 1$, is a solution of the form of a Bessel function of the first kind, $J_1(\left[F_M{}^2 - (1 - \kappa^2)\,F_M - \kappa^2\right]^{1/2}\,\bar{\rho})$ where F_M is some maximum value of F. Equation (11) has been solved numerically (Table 1) and Figure 1 shows the solution for various values of the parameter $K_z = k_z\,V_A/\omega$.

(Table 1)

(Figure 1)

(Figure 2)

The B_θ-field is localized transverse to the background magnetic field line with a characteristic spatial dimension of the order of a few ion Larmor radii. Thus it forms a waveguide along the ambient magnetic field line. By inspection of the far field solution, $K_1(\kappa\bar{\rho})$, we may determine the width of the solitary wave, ρ_M. The value of the argument where the amplitude goes to zero, is given by,

$$\kappa\,\bar{\rho}_M \simeq 3 \qquad (12)$$

from which we obtain

$$\rho_M \simeq 3K_z/(K_z{}^2 - 1)^{1/2} \quad . \qquad (13)$$

Figure 2 shows how the width of the solitary wave varies with K_z. For small amplitude solitary waves, K_z is somewhat larger than unity, and the denominator in Eq. (13) is small. Thus the solitary wave spreads (see Fig. 1). However, as K_z increases, the denominator in Eq. (13) tends toward K_z, and the wave contracts. Thus K_z parametrizes the nonlinearity. The width contracts to its asymptotic value of approximately three ion Larmor radii. The amplitude of the B_θ-field peaks around $\bar{\rho} \sim 1$, and looking along the ambient magnetic field line the solitary wave appears as a ring-shaped region of large magnetic field. This is shown in Fig. 3 where the amplitude of the azimuthal magnetic field B is shown proportional to the density of the circles. In the opposite limit, as κ^2 (and thus the nonlinearity) goes to zero, the solitary wave spreads to infinite width destroying localization, and yielding a plane wave-type solution. As previously shown we may re-write Eq. (11) as

$$\left(\nabla^2 - \frac{1}{\bar{\rho}^2} \right) \tilde{B}_\theta - \tilde{n} \, (K_z^{\,2} - \tilde{n}) \, \tilde{B}_\theta = 0$$

from which it is clear that as n and $K_z^{\,2}$ approach unity, we are left with a linear equation.

(Figure 3)

TABLE I. VALUES OF f FOR $\kappa/K_z = 1.0, 0.7$, AND 0.5 CALCULATED ON THE UNIVERSITY OF MICHIGAN AMDAHL 470 V/6.

Figure 1. Radial Profile of the Azimuthal Amplitude f, for Some Values of κ/K_z, where $\tilde{B}_\theta = f(\kappa\bar{\rho}) \exp(i\kappa\xi)$.

Figure 2. Solitary Wave Width ρ_M as a Function of K_z^2.

Figure 3. Azimuthal Magnetic Field Amplitude in the $\rho - \theta$ Plane Perpendicular to the z-axis. The Ambient Field $\underset{\sim}{B}_o = (0,0,B_o)$ is Directed into the Page. The Amplitude of the Wave Magnetic Field $\underset{\sim}{B} = (0, B_\theta\ (\kappa\bar{\rho}), 0)$ is Shown Proportional to the Density of the Circles.

$\kappa/K_z = 1.0$	$\kappa/K_z = 1.0$	$\kappa/K_z = 0.7$	$\kappa/K_z = 0.5$
ρ	f	f	f
0.00	0.000	0.000	0.000
0.25	0.108	0.048	0.023
0.50	0.225	0.102	0.049
0.75	0.350	0.154	0.082
1.00	0.466	0.210	0.111
1.25	0.499	0.258	0.141
1.50	0.431	0.312	0.173
1.75	0.298	0.321	0.210
2.00	0.201	0.275	0.229
2.25	0.137	0.223	0.248
2.50	0.088	0.181	0.249
2.75	0.042	0.141	0.237
3.00	0.002	0.108	0.212
3.25	0.000	0.077	0.183
3.50	0.000	0.054	0.152
3.75	0.000	0.037	0.126
4.00	-	0.022	0.106
4.25	-	0.011	0.087
4.50	-	0.000	0.069
4.75	-	0.000	0.054
5.00	-	0.000	0.041
5.25	-	-	0.031
5.50	-	-	0.019
5.75	-	-	0.008
6.00	0.000	0.000	0.000

Table 1. Values of f for $\kappa/K_z = 1.0$, 0.7, and 0.5 calculated on the U. of Mich. Amdahl 470 V/6.

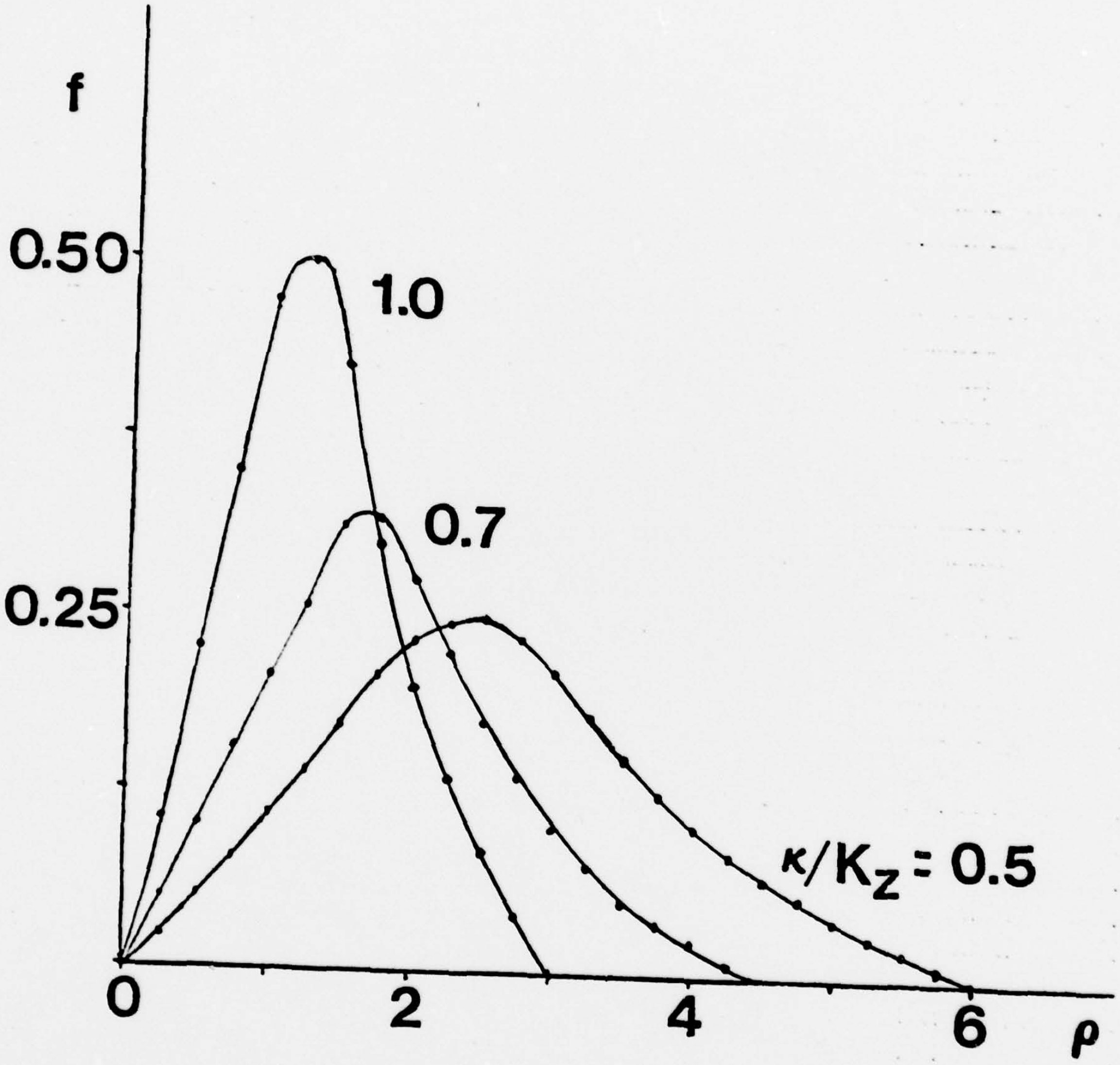

Fig. 1

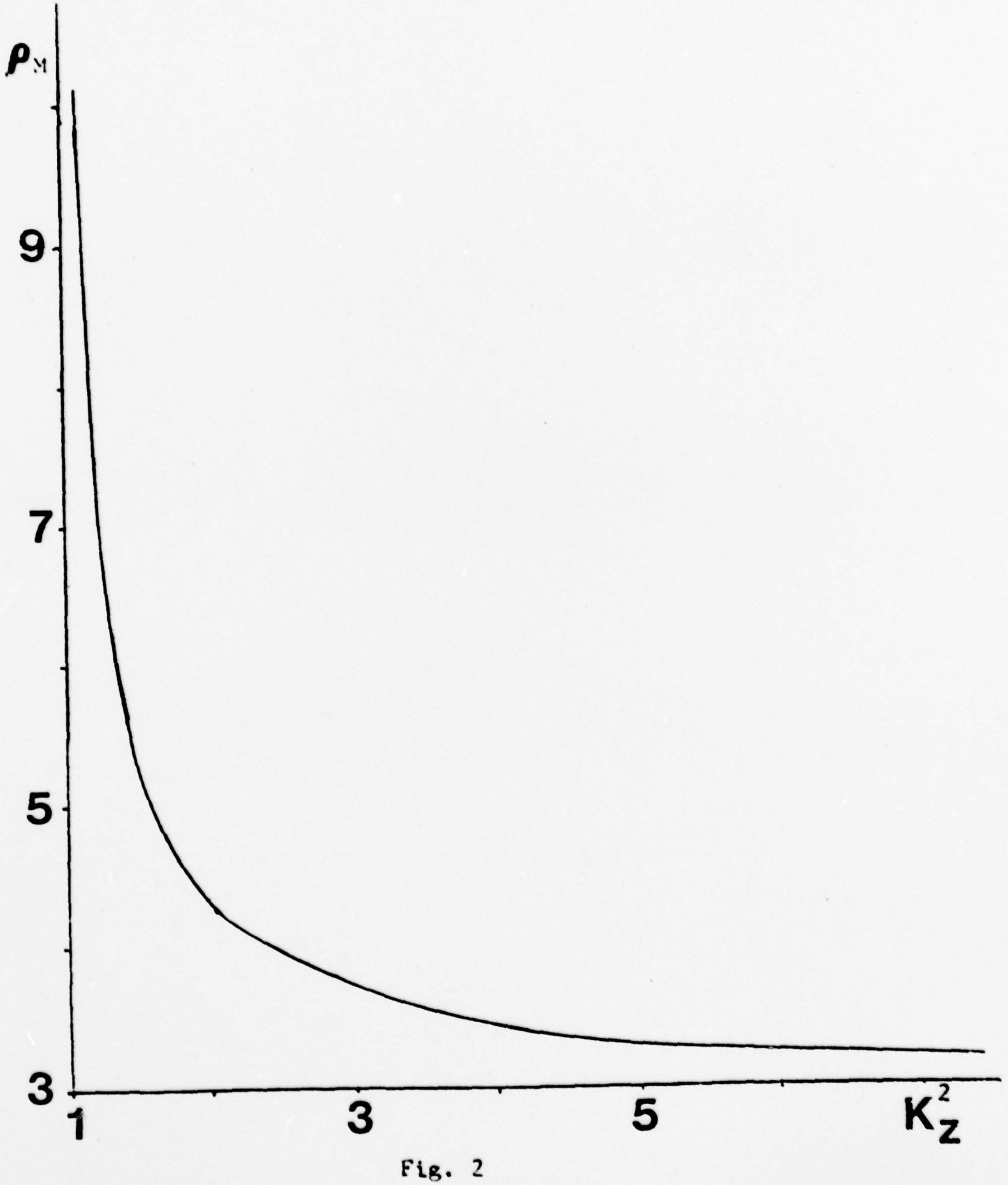

Fig. 2

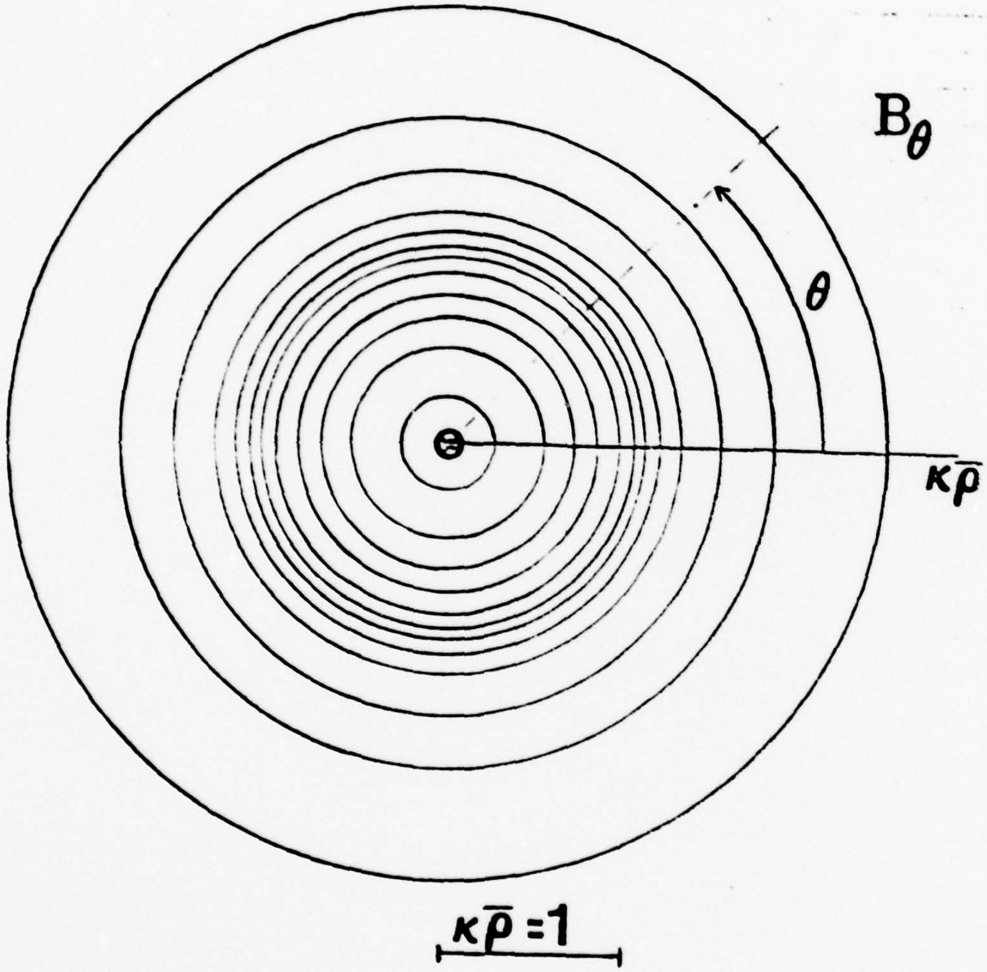

B_θ
θ
$\kappa\bar{\rho}$
$\kappa\bar{\rho} = 1$

Fig. 3

F. COLLISIONAL EFFECTS ON WAVE-BREAKING IN A COLD PLASMA

As the laser beam in our laboratory experiment tunnels its way through the over-dense plasma a large density gradient transverse to the beam is generated. As the plasma is over dense, there exists a region of critical density at some radius r_1, where $0 < r_1 < r_o$, and r_o is the edge of the incident laser beam. In the neighborhood of r_1, the region of critical density, resonant absorption of the laser beam takes place. It is well-known in collisionless plasmas that resonant absorption is one of the effective ways in which an electromagnetic wave can deposit large amounts of energy. In the process a large amplitude electrostatic wave is generated which eventually breaks with the consequent production of energetic (suprathermal) electrons. Ion dynamics and thermal effects modify the wa-e breaking amplitude. They reduce the role of the wave-breaking process of energy dissipation by providing competing modes of energy release. Collisions produce a similar effect. As our laboratory plasma is very dense and has a relatively low temperature, collisional effects are important. Therefore we investigate its effect on the wave-breaking amplitude.

Consider an electromagnetic wave incident upon a plasma with a linear density profile. Let E_d be the component of the incident wave electric field parallel to the density gradient. A Lagrangian formalism will be used to describe the nonlinear electron plasma oscillations under the influence of the driver field E_d. From the equation of motion of the electrons (including the collision term) and Poisson's equation it is found that the electron displacement δ satisfies

$$\ddot{\delta} + \nu\dot{\delta} + \omega_{pe}^{2}(x_o)\,\delta = \varepsilon \sin t \tag{F-1}$$

where $\varepsilon = e\,E_d/m_e\,\omega_d^2\,L$; ω_d is the frequency of the incident electromagnetic wave; L is a characteristic distance, e.g., the density gradient scale length. All distances and times in Eq. (F-1) are normalized with respect to L and ω_d^{-1} respectively. Thus Eq. (F-1) is an equation in dimensionless form. The effect of collisions is taken into account by the second term in Eq. (F-1) where ν is proportional to the electron-ion collision frequency. The displacement of an electron initially at position x_o is given by δ, i.e.

$$\delta(x_o,t) = x(t) - x_o \quad . \tag{F-2}$$

It has been implicitly assumed in Eq. (F-1) that $\delta << 1$.

The solution of Eq. (F-1) is given by (see Appendix)

$$\begin{aligned}\delta(t) = {} & [e/\cos\gamma\,(\omega_p^2 - 1 + \nu\tan\gamma)]\,[\exp(-\nu t/2)] \\ & \Big\{(\sin\gamma)\cos\Big[\big(\omega_p^2 - \tfrac{1}{4}\nu^2\big)^{1/2}t\Big] \\ & + \big(\tfrac{1}{2}\nu\sin\gamma - \cos\gamma\big)\sin\Big[\big(\omega_p^2 - \tfrac{1}{4}\nu^2\big)^{1/2}t\Big]/\big(\omega_p^2 - \tfrac{1}{4}\nu^2\big)^{1/2}\Big] \\ & + \sin(t-\gamma)\Big\}\end{aligned} \tag{F-3}$$

where $\gamma \equiv \tan^{-1}(\nu/\omega_p^2 - 1)$. Let us now consider the behavior of $\delta(t)$ at the resonance region where the electrostatic wave grows most rapidly. We take the limit as $\omega_p \to 1$ and let $\nu^2 << \omega_p^2$. The result is

$$\delta(t) = (\varepsilon/\nu)\Big\{\exp(-\nu t/2)\big(\cos t + \tfrac{1}{2}\nu\sin t\big) - \cos t\Big\} \tag{F-4}$$

Note the limiting effect that the exp $(-\nu t/2)$ factor has on the wave amplitude. Clearly, for sufficiently large values of ν the electrostatic wave is drastically modified. It is also to be observed that in the limit $\nu \rightarrow 0$ the collisionless result of Koch and Albritton is recovered.

In order to examine the effect of the collision frequency in more detail we consider the time t_b at which the wave breaks. This condition occurs when $\partial\delta/\partial x_o = -1$, i.e., when the electron paths cross one another. We now apply this condition to Eq. (F-4) and find that t_b satisfies the relation

$$\nu^2/\varepsilon = 1 - \exp\,(-\,\nu t_b/2)\left(1 + \frac{1}{2}\,\nu t_b\right) \quad . \qquad \text{(F-5)}$$

This relation is shown graphically in Fig. 1. The important thing to note is that the right hand side is never larger than unity. Thus, if $\nu > \varepsilon^{1/2}$, the electrostatic wave cannot break. Instead of the wave to break and disperses its energy into hot electrons that stream out of the region, the electron-ion collisions thermalize the wave energy in the resonance region.

Thus to prevent wave-breaking the electron-ion collision frequency has to exceed $(e\,E_d/m_e\,\omega_d^{\,2}L)^{1/2}$. For lower values of ν the wave does break, but is now modified by collisions. Aside from the much longer breaking time, the resulting electron velocity V_c is also reduced. The electron velocity at wave-breaking V_c is obtained by taking the time-derivative of δ in (F-4) and evaluating it at $t = t_b$. Figure 2 shows the electron velocity at wave-breaking as a function of the collision frequency. Thus collisions can significantly reduce the energy carried away by the hot electrons.

Finally, the limitations of this analysis need to be pointed out. With the longer wave-breaking times the effect of ion bunching becomes more important. However, this can be offset somewhat by consideration of ion collisions. Furthermore, as collisions have the effect of thermalizing the wave energy in the resonance region, temperature effects would also become significant. Finally, it is tacitly implied in the above analysis that $\nu t > 1$, i.e., the electrons suffer at least one collision before the wave breaks.

(Figure)

(Figure)

APPENDIX (to Section F)

Consider the equation

$$\ddot{\delta} + \nu\dot{\delta} + \omega_{pe}(x_o)\,\delta = \varepsilon \sin t \qquad \text{(F-A.1)}$$

The general solution of the associated homogeneous equation is, assuming $\omega_p^2 > \frac{1}{4}\nu^2$,

$$\delta_H = \exp\left(-\frac{1}{2}\nu t\right)\left[c_1 \cos\left\{\left(\omega_p^2 - \frac{1}{4}\nu^2\right)^{\frac{1}{2}} t\right\} + c_2 \sin\left\{\left(\omega_p^2 - \frac{1}{4}\nu^2\right)^{\frac{1}{2}} t\right\}\right]$$

with c_1 and c_2 to be determined from the initial conditions.

To find a particular solution of the nonhomogeneous equation, (F-A.1), we try

$$\delta_p = c_3 \sin(t - \gamma) \quad .$$

Substituting this into (F-A.1) and setting the coefficients of the sin t and cos t terms equal to zero we obtain

$$\gamma = \tan^{-1}\left[\nu/(\omega_p^2 - 1)\right]$$

$$c_3 = \varepsilon/\cos\gamma\,(\omega_p^2 - 1 + \nu\tan\gamma) \quad .$$

Thus the solution so far is

$$\delta(t) = (c_1 \cos\alpha t + c_2 \sin\alpha t)\exp\left(-\frac{1}{2}\nu t\right) + c_3 \sin(t - \gamma)$$

with c_3 and γ defined above and $\alpha = \left(\omega_p^2 - \frac{1}{4}\nu^2\right)^{\frac{1}{2}}$. We now determine c_1 and c_2 from the initial conditions

$$\delta(t=0) = 0 \quad , \quad \dot{\delta}(t=0) = 0$$

The final form of the solution is then given by

$$\delta(t) = \left\{\varepsilon/\cos\gamma\,(\omega_p^{\,2} - 1 + \nu\tan\gamma)\right\} \cdot$$

$$\cdot \left\{ \exp(-\nu t/2)\left[\sin\gamma\cos\left\{\left(\omega_p^{\,2} - \frac{1}{4}\nu^2\right)^{\frac{1}{2}} t\right\}\right.\right.$$

$$\left.\left. + \left(\frac{1}{2}\nu\sin\gamma - \cos\gamma\right)/\sin\left\{\left(\omega_p^{\,2} - \frac{1}{4}\nu^{2\,\frac{1}{2}}\right)t\right\}\Big/\left(\omega_p^{\,2} - \frac{1}{4}\nu^2\right)^{\frac{1}{2}}\right.\right. + \sin(t - \gamma)$$

This is Eq. (F-3) in the text.

If we further make the assumption that $\omega_p^{\,2} >> \frac{1}{4}\nu^2$, then we have

$$\delta(t) = \left\{\varepsilon/\cos\gamma\,(\omega_p^{\,2} - 1 + \nu\tan\gamma)\right\} \cdot$$

$$\cdot \left\{(\exp(-\nu t/2)\left[\sin\gamma\cos\omega_p t\right.\right.$$

$$\left.\left. + \left(\frac{1}{2}\nu\sin\gamma - \cos\gamma\right)(\sin\omega_p t)/\omega_p\right]\right. + \sin(t - \gamma)$$

At resonance, $\omega_p \rightarrow 1$,

$\tan\gamma = \dfrac{\nu}{\omega_p^{\,2} - 1} \rightarrow \pm\infty$ and $\gamma \rightarrow \pm\pi/2$. Hence, at resonance,

$$\delta(t) = (\varepsilon/\nu)\left\{\exp(-\nu t/2)\left(\cos t + \frac{1}{2}\nu\sin t\right) - \cos t\right\} .$$

This is Eq. (F-4) in the text.

Figure . The right hand side of the relation

$$\nu^2/\varepsilon = 1 - \exp\left(-\frac{1}{2}\nu t_b\right)\left(1 + \frac{1}{2}\nu t_b\right)$$

plotted as a function of the wave-breaking time. The dotted curve shows the wave-breaking time in the absence of collisions.

Figure . The electron velocity at wave-breaking versus the (scaled) collision frequency. $V_o = (2\varepsilon)^{\frac{1}{2}}$ is the electron velocity at wave-breaking in the case of a collisionless plasma.

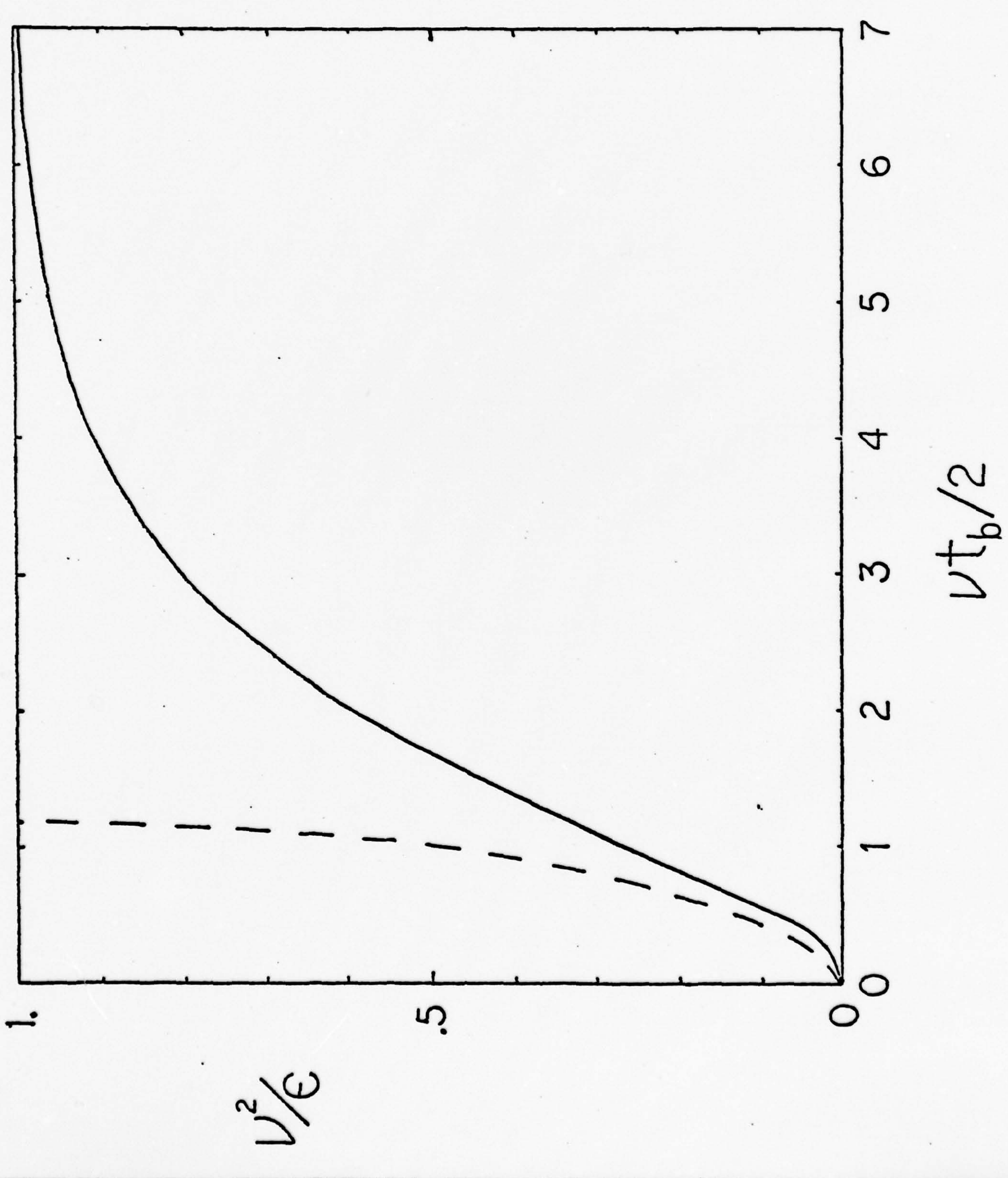
ν^2/ϵ
1.
.5
0
0
1
2
3
4
5
6
7
$\nu t_b/2$

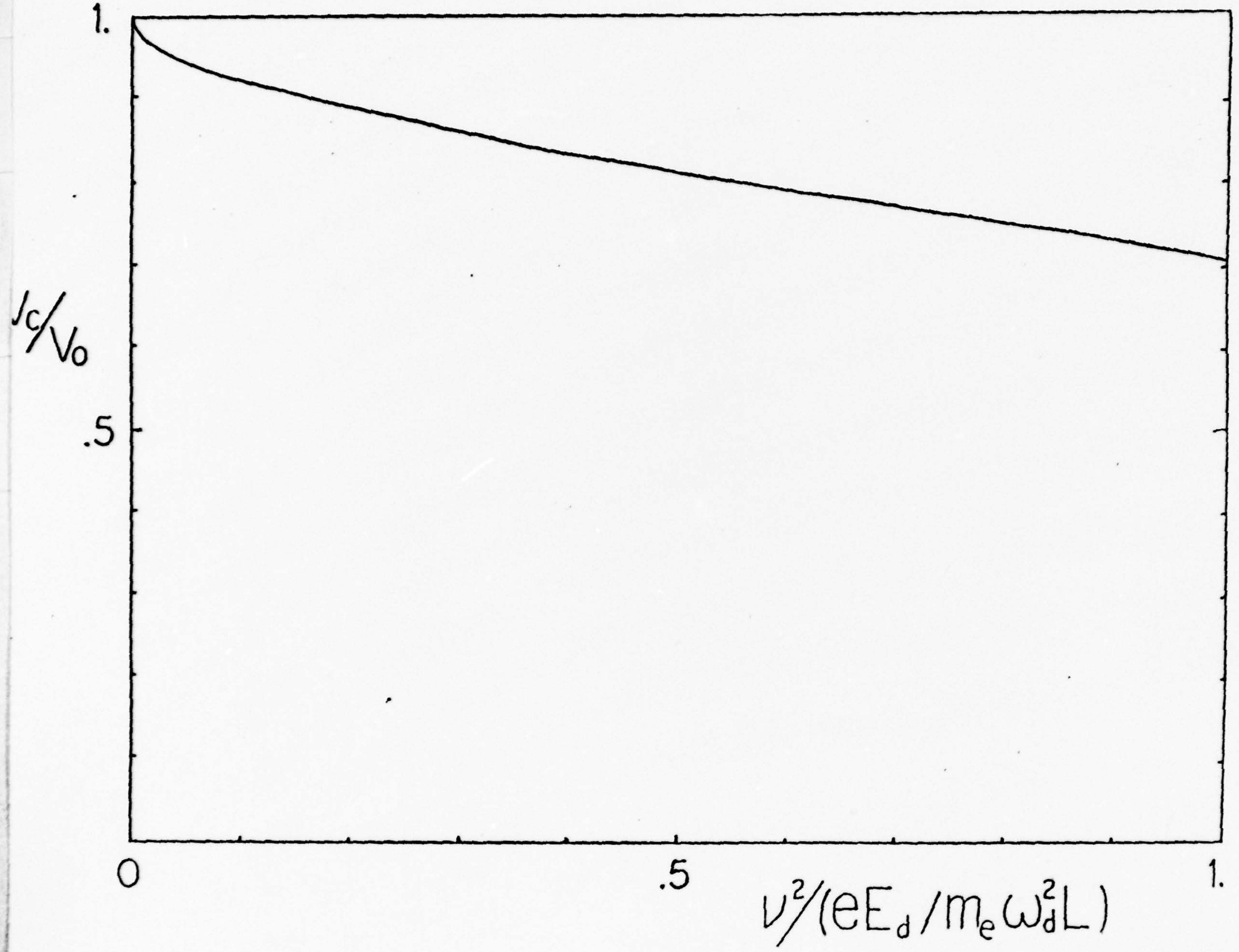
1.
.5
c/Vo
0
.5
1.
ν²/(eE_d /m_e ω_d²L)

G. STUDIES OF RANDOM PERTURBATIONS ON PARAMETRIC EXCITATION PROCESSES

One of the more popular explanations for the anomalously strong interaction which is observed between intense laser light and plasmas involves the excitation of parametric instabilities in the plasma. The high frequency electromagnetic field of the incident laser beam couples with the natural modes of the target plasma (e.g., electron plasma waves or ion-acoustic waves) and drives them unstable. Such instabilities will eventually saturate in a turbulent plasma state which characterizes the further interaction.

The two simplest models of such parametric process involve the parametric excitation of simple harmonic oscillators:

i) Single-mode parametric excitation

$$\frac{d^2X}{dt^2} + 2\Gamma \frac{dX}{dt} + \Omega^2 X(t) = 0 \qquad \text{(G-1)}$$

where the excitation enters through the frequency

$$\Omega^2 = \Omega_o^2 (1 - 2\varepsilon \cos \omega_o t) \qquad \text{(G-2)}$$

ii) Coupled-mode parametric excitation

$$\begin{aligned} \frac{d^2X_1}{dt^2} + 2\Gamma_1 \frac{dX_1}{dt} + \omega_1^2 X_1(t) &= \lambda_1 Z(t) X_2(t) \\ \frac{d^2X_2}{dt^2} + 2\Gamma_1 \frac{dX}{dt} + \omega_1^2 X_2(t) &= \lambda_2 Z(t) X_1(t) \end{aligned} \qquad \text{(G-3)}$$

where $Z(t) = Z_o/2 \cos \omega_o t$; ω_1, ω_2 are natural oscillation frequencies; and ω_o is the pump frequency. In this latter model, one expects strong resonant energy transfer between the pump (e.g., incident laser beam) and the natural oscillations when $\omega_o \sim \omega_1 + \omega_2$. Hence in the usual analysis, one assumes that

a) a resonance condition is satisfied: $\omega_o \sim \omega_1 + \omega_2$

b) both the pump and the damping are weak: $\varepsilon << 1$, $\Gamma << \omega$.

The general approach in analyzing parametric processes in plasmas is now to cast the relevant equations describing the driven plasma (e.g. the hydrodynamics equations) into one of these forms, and then determine the threshold and growth rates of any parametric instabilities which may arise.

In any actual interaction process, there will be a certain amount of "noise" which can significantly affect the coupling between the pump and the natural oscillations. For example, if the pump (laser beam) has passed through a turbulent medium, it will be characterized by a random phase variation. Furthermore, most incident laser beams are not monochromatic, but rather may exhibit an almost random frequency modulation as well as a random amplitude variation. To investigate the implications of such noise on parametric processes, we are applying several recent developments from the theory of stochastic differential equations.

The general structure of such theories seeks to arrive at an approximate equation for the mean solution $\langle u(t)\rangle$ of a general differential equation of the form

$$\frac{\partial u}{\partial t} = L(t)\ u(t) \qquad \text{(G-4)}$$

where $L(t)$ is a general stochastic operator which can be separated into mean and fluctuating components as $L(t) \equiv \langle L(t)\rangle + \delta L(t)$. One of the most popular theories is based upon the Bourret approximation in which $\langle u(t)\rangle$ is described by an approximate equation of the form

$$\frac{\partial\langle u\rangle}{\partial} \quad \langle L(t)\rangle\langle u(t)\rangle \quad \int_{t_o}^{t} dt_1 \, \langle \delta L(t) \; u(t,t_1) \; \delta L(t_1)\rangle\langle u(t_1)\rangle \tag{G-5}$$

where the propagator $u_o(t,t_o)$ is described by

$$\frac{\partial u_o}{\partial t} - \langle L(t)\rangle \; u_o(t,t_o) = 0 \qquad , \qquad u(t_o,t_o) = 1 \tag{G-6}$$

By way of example, if we consider single mode parametric excitation (ignoring damping for convenience)

$$\frac{d^2X}{dt^2} + \Omega^2(t) \; X(t) = 0 \tag{G-7}$$

and allow the frequency $\Omega^2(t)$ to possess a random component $\xi(t)$

$$\Omega^2(t) = \Omega_o{}^2 - 2\varepsilon \; \Omega_o{}^2 \cos \omega_o t + \varepsilon\xi(t) \tag{G-8}$$

then in the weak pump limit we find that the Bourret approximation yields an equation for the mean

$$\frac{d^2\langle x\rangle}{dt^2} + \frac{1}{2}\,\varepsilon^2 \, C_2 \, \frac{\overset{2}{d}\langle x\rangle}{dt^2} + \left[\Omega_o{}^2 \; (1 - 2\varepsilon \cos \omega_o t) - \frac{1}{2}\,\varepsilon^2 \, C_1\right] \langle X(t)\rangle = 0 \tag{G-9}$$

where

$$C_1 \equiv \int_0^\infty \langle \xi(t) \;\; \xi(t - \tau \rangle \; \sin 2\tau d\tau$$

$$C_2 \equiv \int_0^\infty \langle \xi \; (t) \;\; \xi(t - \tau)\rangle \; (1 - \cos 2\tau) \; d\tau$$

Hence a random frequency component is seen to cause both a damping as well as a frequency shift.

A second example would be coupled-mode parametric excitation with a randomly modulated pump

$$Z(t) = \frac{Z_o}{2}\,\xi(t)\cos\omega_o t \qquad \text{(G-10)}$$

If we utilize the resonance conditions and the Bourret approximation, we find that the random pump changes the instability threshold condition from

$$\frac{Z_o^{\,2}\,\lambda_1\lambda_2}{4} = \Gamma_1\Gamma_2 \qquad \text{(deterministic pump)} \qquad \text{(G-11)}$$

to

$$\frac{Z_o^{\,2}\,\lambda_1\lambda_2}{4\,\Delta\omega} = \min\,(\Gamma_1,\Gamma_2) \qquad \text{(random pump)} \qquad \text{(G-12)}$$

that is, the presence of noise raises the threshold by a factor $\Delta\omega/\min\,(\Gamma_1,\Gamma_2)$ where $\Delta\omega$ is the spectral width of the noise. In this particular example, the noise actually decouples the natural modes.

H. DEVELOPMENT OF MHD PLASMA SIMULATION MODELS

In order to understand the complex dynamics of nonequilibrium plasmas interacting with laser radiation, one must take into account the hydrodynamic motion of these plasmas as they are produced, heated, and expand into the target chamber. Of particular concern here is the theoretical investigation of the relative significance of various types of energy absorption and transfer mechanisms as well as the interpretation of experimental data. For that reason we have placed a high priority on the development of MHD computer codes capable of simulating exploding wire or pinch dynamics when subjected to intense laser irradiation. Most of our effort in this direction over the past year has involved the development of nonequilibrium models to describe the ionization dynamics and radiation emission from dense, metallic plasmas of low to moderate atomic number.

This work has been stimulated in part by the interest in exploding wire devices as intense X-ray sources or in using dense metallic plasmas to convert long wavelength laser radiation into X-rays (using line emission). For elements of medium-to-large atomic number, Z, the ion species consisting of only one or two inner shell electrons are excellent discrete X-ray emitters, since their bound state transition energies from excited to ground level scales as Z^2 times the energies of hydrogen transitions. It is these transitions which are the source of most of the discrete X-ray emission from exploding wire plasmas.

An MHD computer code forms the basis for our simulation studies in which the macroscopic plasma parameters are determined as a function of time and radius in a one-dimensional, cylindrically symmetric configuration (see Table H-1 for the relevant equations). The ionization

TABLE H-1. MHD PLASMA MODEL

$$\frac{Dv}{Dt} = v\underline{\nabla} \cdot \underline{u}$$

$$\frac{Du}{Dt} = v\underline{\nabla}(p + q) + v(\underline{J} \times \underline{H})$$

$$\frac{De_e}{Dt} = - vP_e\underline{\nabla} \cdot \underline{u} + v\underline{\nabla} \cdot (\kappa_e\underline{\nabla}\, T_e) - \frac{R}{\gamma - 1}\,\frac{(T_e - T_i)}{t_{eq}} + S$$

$$\frac{De_i}{Dt} = - v(P_i + q)\ \underline{\nabla} \cdot \underline{u} + v\underline{\nabla} \cdot (\kappa_i\underline{\nabla}\, T_i) + \frac{R}{\gamma - 1}\,\frac{(T_e - T_i)}{t_{eq}}$$

$$\underline{\nabla} \times \underline{E} = - \frac{\partial H}{\partial t}$$

$$\underline{\nabla} \times \underline{H} = 4\pi\underline{J} + \frac{1}{c^2}\,\frac{\partial E}{\partial t}$$

$$\eta\underline{J} = \underline{E} + \underline{u} \times \underline{H}$$

$$P_\alpha v = Z_\alpha\, RT_\alpha \qquad\qquad e_\alpha = \frac{Z_\alpha R}{\gamma - 1}\, T_\alpha$$

Here α = e, i, v is specific volume, $\underline{u}$ is velocity, q is the usual artificial viscosity term, κ is thermal conductivity, t_{eq} is equipartition time, $\underline{J}$ is current density, $\underline{H}$ and $\underline{E}$ are magnetic and electric field intensities, p is pressure, η is resistivity, e is internal energy, and Z is charge state. The term, S, contains the plasma energy source and loss terms,

$$S = \Psi - \frac{\partial E_I}{\partial t} - R + Q_\ell$$

where Ψ is Joule heating, R is radiation emission, dE_I/dt is energy lost due to ionization of the plasma, and Q_ℓ is the laser energy addition term. The expressions for the thermal conductivities are taken from Braginskii, while the resistivity and equipartition time are taken from Spitzer.

and radiation dynamics of dense, magnetohydrodynamic plasmas has been modeled in a fashion suitable for implementation in MHD computer simulation codes. It has been shown that more primitive LTE models such as those based on the Saha equation are inadequate to describe the rapidly varying temperature and density regimes characterizing many such plasmas. Both the assumptions of thermodynamic equilibrium in the plasma and the neglect of radiative recombination in determining the effective plasma charge state and density distribution of ions among the various states are invalid for these plasmas. By direct comparison of theoretical calculations based upon the LTE model with those obtained from the more sophisticated model based upon time dependent rate equations employing atomic cross-sectional data, and also by comparison of predicted line ratios with actual experimental data, we have shown that the latter model is necessary for an accurate estimate of plasma ionization dynamics.

Detailed collisional-radiative models are developed which directly solve the time-dependent rate equations characterizing atomic processes along with those equations characterizing the hydrodynamic motion of the plasma. These models are applied to analyze high density helium Z-pinch and lithium exploding wire plasmas, and they are found to yield results which compare quite favorably with experimental data.

A theoretical model of the magnetohydrodynamic (MHD) motion and radiation emission characterizing dense, laser-heated exploding wire plasmas has been developed which solves (numerically) the set of MHD equations coupled with a set of atomic rate equations describing the ionization and radiation dynamics of the plasma. The model has been applied to study the use of a high powered laser to ionize and heat an aluminum exploding wire plasma. Particular attention has been directed towards the radiation emission from such a plasma which includes free-free (bremsstrahlung), free-bound (radiative recombination), and bound-bound (line emission) contributions. Included in the line emission are hard X-rays produced by excited level-to-ground state transitions in the helium-like and hydrogen-like ion species.

Laser absorption efficiency and laser-to-X-ray conversion efficiencies have been studied as functions of laser pulse width, laser intensity, and initial wire diameter. It was found that the X-ray emission depends critically on the laser intensity, the plasma density profile and hydrodynamic motion at the time of laser interaction, and the strength of the plasma current and its subsequent self-consistent, confining magnetic field.

In addition, the importance of the exploding wire dynamics in relation to the subsequent radiation emission was demonstrated by comparing the data on two experiments in which the initial time of laser incidence differed. More specifically, it was shown that modifying the density profile, initially, for strong laser abosrption does not assure what the laser energy addition will be converted to X-ray emission with maximum efficiency. A careful balance of the hydrodynamic motion is required for peak conversion; hence, care must be taken when choosing the value of the maximum current and its frequency used to explode the wire. Even then, the choice of the appropriate pinch and the particular time before that pinch at which to trigger the laser may critically determine the laser-to-X-ray conversion efficiency.

It appears that the confining magnetic fields might be exploited to contain the plasma at constant densities while laser heating takes place. The higher fields corresponding to the later time for laser incidence (hence, higher current from the sine-wave) in the 1 mil wire simulations, no doubt, played a significant role in the higher efficiency of X-ray production obtained in that study. A modified current profile that increases dramatically in a step or ramp function after laser heating begins might produce this confinement.

I. EXTERNAL CIRCUIT EFFECTS ON PLASMA DYNAMICS

Our hydrodynamic simulation models were modified to include a self-consistent treatment of the coupling of the plasma to an external circuit. Here we followed closely the procedure used in the WHYRAC code developed at the Naval Research Laboratory. This treatment models the external circuit as a driving voltage into an effective lumped circuit characterized by resistance and inductance. The plasma is then treated in an exact fashion as a distributed circuit element using the MHD model. An iterative procedure is employed to solve the coupled circuit equations.

We have compared MHD calculations of the dynamics of a fast Z-pinch helium plasma both with and without coupling to an external circuit in Figures 1 and 2. In the latter calculation the total current through the plasma is specified as a sin shape in time. Although several detailed features of the plasma dynamics are modified slightly by the inclusion of external circuit effects (notably pinch time, peak density, and peak temperature), the general features remain unchanged.

Plasma density versus radius and time for a fast z-pinch helium plasma: (a) sin shape current (b) with external circuit calculation.

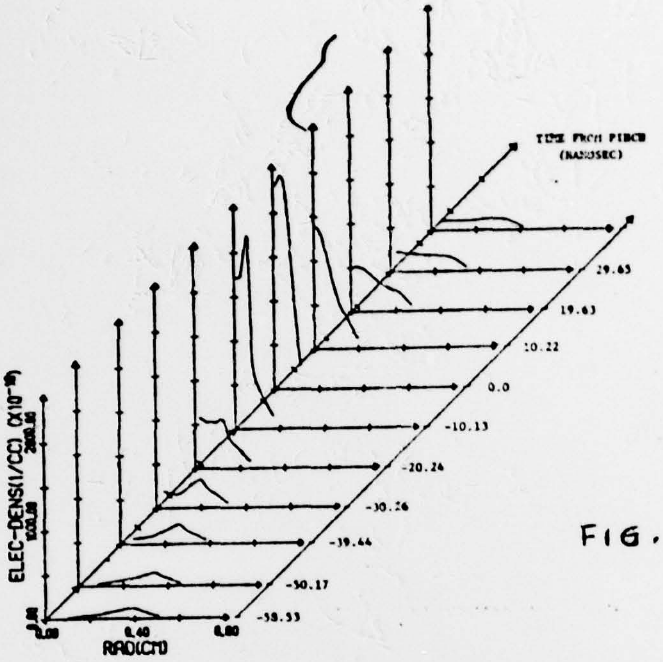

FIG. 1

(a) sin shape current

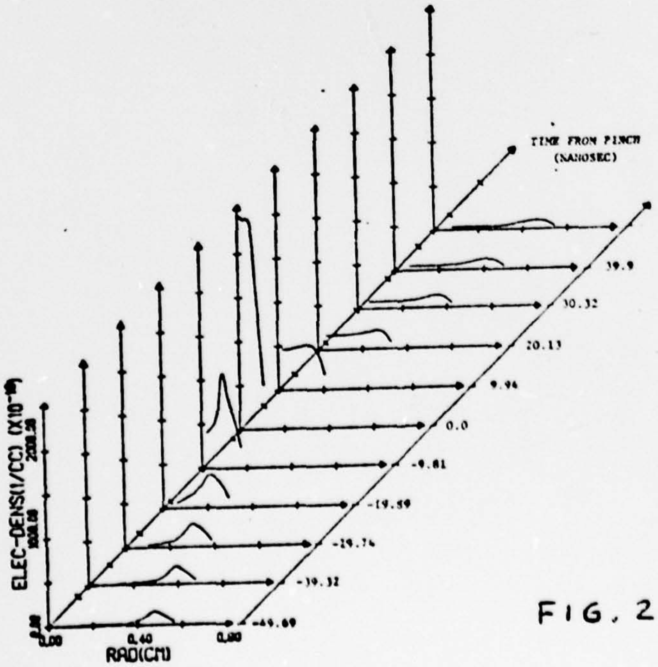

FIG. 2

(b) with external circuit

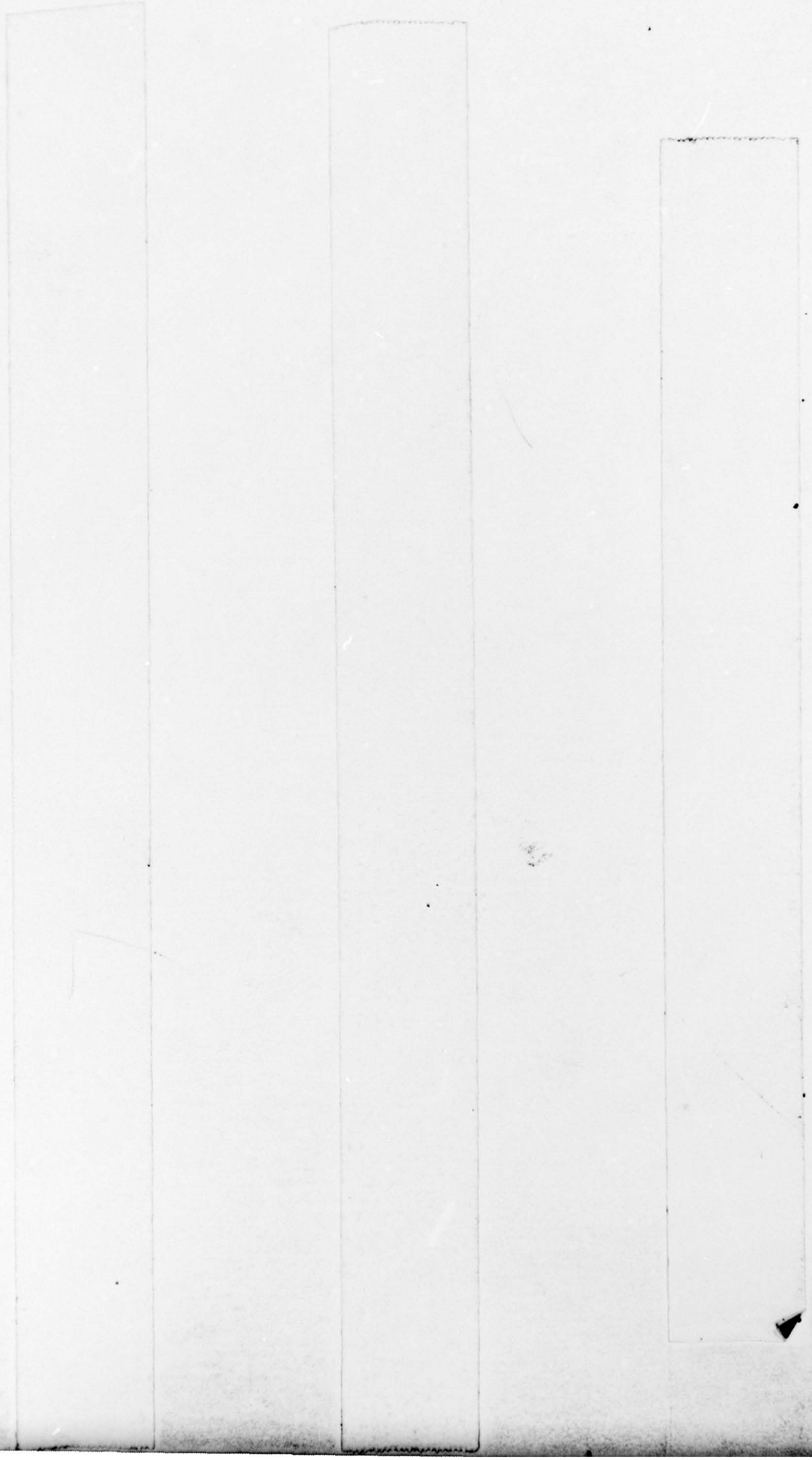

J. TRANSVERSE EFFECTS ON LASER BEAM PROPAGATION IN PLASMAS

The laser-plasma interaction experiments performed in our laboratory indicate that an intense CO_2 laser beam can actually penetrate through an over-dense plasma column. A theory based on nonlinear optical effects due to nonuniform transverse temperature and density profiles across the beam appears to explain many of the experimentally observed characteristics of this phenomenon. However we also analyzed this process from a somewhat different perspective by making use of a plasma hydrodynamics computer code equipped with a laser light propagation and interaction package.

More specifically, we modified the laser-plasma hydrodynamics computer code PHD to analyze laser beam propagation through an over-dense plasma. The PHD code solves the one fluid, two temperature equations of hydrodynamics in one-dimensional (slab, cylindrical, and spherical) geometry in Lagrangian coordinates. The momentum equation is solved using an explicit finite difference technique with the addition of artificial viscosity. The energy equations include flux-limited thermal diffusion through the electrons and ions, work on the electrons and ions, collisional coupling between the electrons and ions, and source therms. The electron source term is due to laser light absorption calculated using inverse bremsstrahlung coefficients. Laser beam propagation is analyzed by solving the relevant photon transport equations.

The original version of the PHD code was not directly applicable to the problem of interest because it is restricted to one-dimensional symmetry and does not take account of magnetic fields. However we modified the code to include an approximate treatment of these effects. In particular, we added terms to account for magnetic pressure effects. We have modified transport coefficients (most notably, thermal conductivity) to account for magnetic fields. Cyclotron radiation loss terms are also included. To account for transverse effects, we have included artificial source sink terms in the hydrodynamics equations to account for transverse heat conduction and mass flow.

Our "1.5-D" hydrodynamic model explains several features of the experiment. In particular, the time required for beam penetration, the transmitted laser pulse shape, and the basic characteristics of the density profile are in good agreement with the experimental observations.

K. TRANSPORT PROCESSES IN DENSE PLASMAS

It has become apparent from both experimental measurements and computer plasma simulation studies that non-hydrodynamic transport processes can play a major role in the dynamics of dense plasmas. One must provide a satisfactory treatment of radiation transport effects in any theoretical model of the plasma. Of particular concern here are X-ray line emission, transport, and re-absorption in optically thick regions of the plasma. But situations can also arise, particularly in laser heated plasmas, when the transport of non-thermal charged particles (primarily electrons) can dominate the plasma behavior.

Therefore, we turned our attention to studies of how one can adequately account for such transport processes within a hydrodynamic model of the plasma. Here, we relied heavily on our experience with very similar problems which arise in the study of neutron transport in fission chain reaction systems.

1. Charged Particle Transport

The accurate simulation of the transport of energetic (i.e. superthermal) charged particles is of vital importance to the success of many controlled thermonuclear fusion schemes. For example, there has been great interest in simulating the transport of superthermal electrons during the implosion process in inertial confinement schemes (notably laser fusion) as well as investigating burn-wave propagation via the deposition of the 3.5 MeV alpha particle energy in the dense core of a compressed microsphere. In inertial confinement schemes using either electrons or ions, there are many questions to be studied concerning the deposition of the charged particle energy in the target, the propagation of beams through space-charge neutralizing media, and the like, that likewise require an accurate simulation of energetic charged particle transport. Charged particle transport also plays a fundamental role in areas of plasma physics. For example, there is considerable intere-t in obtaining solutions of the spatially inhomogeneous Fokker-Planck equation to study the energy deposition from neutral beam injection into Tokamak devices where the ionized beam particles are either directly injected or scattered into trapped orbits.

The interaction mechanism of most concern in the transport of energetic charged particles in plasmas involves small angle scattering collisions.

The most common description of the cumulative effect of many random, small angle collisions on a distribution of particles is provided by the Fokker-Planck equation. Since Fokker-Planck equation is commonly used as the basis for most numerical studies of charged particle transport in plasmas, a variety of methods have been developed to solve it. In much of the early work such as that developed for modeling magnetic mirror devices the spatial dependence was suppressed and only the velocity space physics was retained. More recent methods which specifically account for spatial effects include modified multigroup flux-limited diffusion schemes and the integral particle tracking techniques. However, most of these schemes involving the introduction of substantial approximations into the Fokker-Planck equation in order to arrive at a set of equations that are amenable to numerical solutions.

We have developed a direct numerical approach which solves the Fokker-Planck equation in full generality including time, space, and velocity dependence. This scheme can easily be generalized to include more sophisticated physics in the future. To this end, we relied on the discrete ordinates method since it is the most highly developed numerical technique for obtaining deterministic solutions to the transport equation.

The use of the discrete ordinate method for solving the spatially-dependent Fokker-Planck equation is particularly attractive since it has been highly developed for the solution of radiation transport problems. Indeed, there are a variety of sophisticated and efficient one and two dimensional computer codes available that have planar, cylindrical, and spherical geometry options (as well as toroidal and triangular meshes for non-orthogonal geometries) and allow for a variety of boundary and source conditions. Therefore, the successful incorporation of the Fokker-Planck collision term into the multigroup discrete ordinates formalism provides for an easy extension to a variety of geometries and source configurations.

We implemented our numerical procedure for solving the Fokker-Planck equation by modifying a versatile time-dependent discrete ordinates code, TIMEX, to allow for the Fokker-Planck collision term. TIMEX is a time-dependent particle transport code originally develope for the study of neutron transport. It utilizes a discrete ordinates treatment of the particle direction (angle), a discontinuous, linear finite element treatment of the spatial variable, a multigroup treatment of the energy variable, and an explicit time differencing scheme.

The suitability of these features for the analysis of charged particle transport will become apparent as we proceed with our development. We refer to the modifications of this code as TIMEX-FP. Typical results are provided in Fig. 2.

As far as we know, the TIMEX-FP code represents the most complete attempt at solving the space, time, angle, and energy-dependent Fokker-Planck equation to date. We have attempted to retain as much of the original physics content of the equation as possible and have indicated that genearlizations to include nonlinearities or spatial inhomogeneities should be easily accomplished within the established formalism. Moreover, the successful application of established multigroup discrete ordinates techniques has obviated the need for independent and redundant development of the large variety of geometyr, boundary, and source configurations that are immediately available in a large number of stock production discrete ordinates codes.

It has been demonstrated that the discrete ordinates method is capable of accurately modeling the full range of the Fokker-Planck collisional physics without recourse to any significant approximations. Therefore, it should provide a useful tool for studying the details of many plasma physics problems where, for example, a knowledge of the time dependent evolution of the single particle distribution function or the spatial dependence of the energy deposition profile is desired.

2. Photon Transport in Dense Plasmas

In recent years there has been considerable interest in X-ray emissions from laser fusion plasmas and dense, metallic plasmas. Our early hydrodynamic simulation models have been limited by the assumption that the plasmas is transparent to all line radiation. The

Figure 2

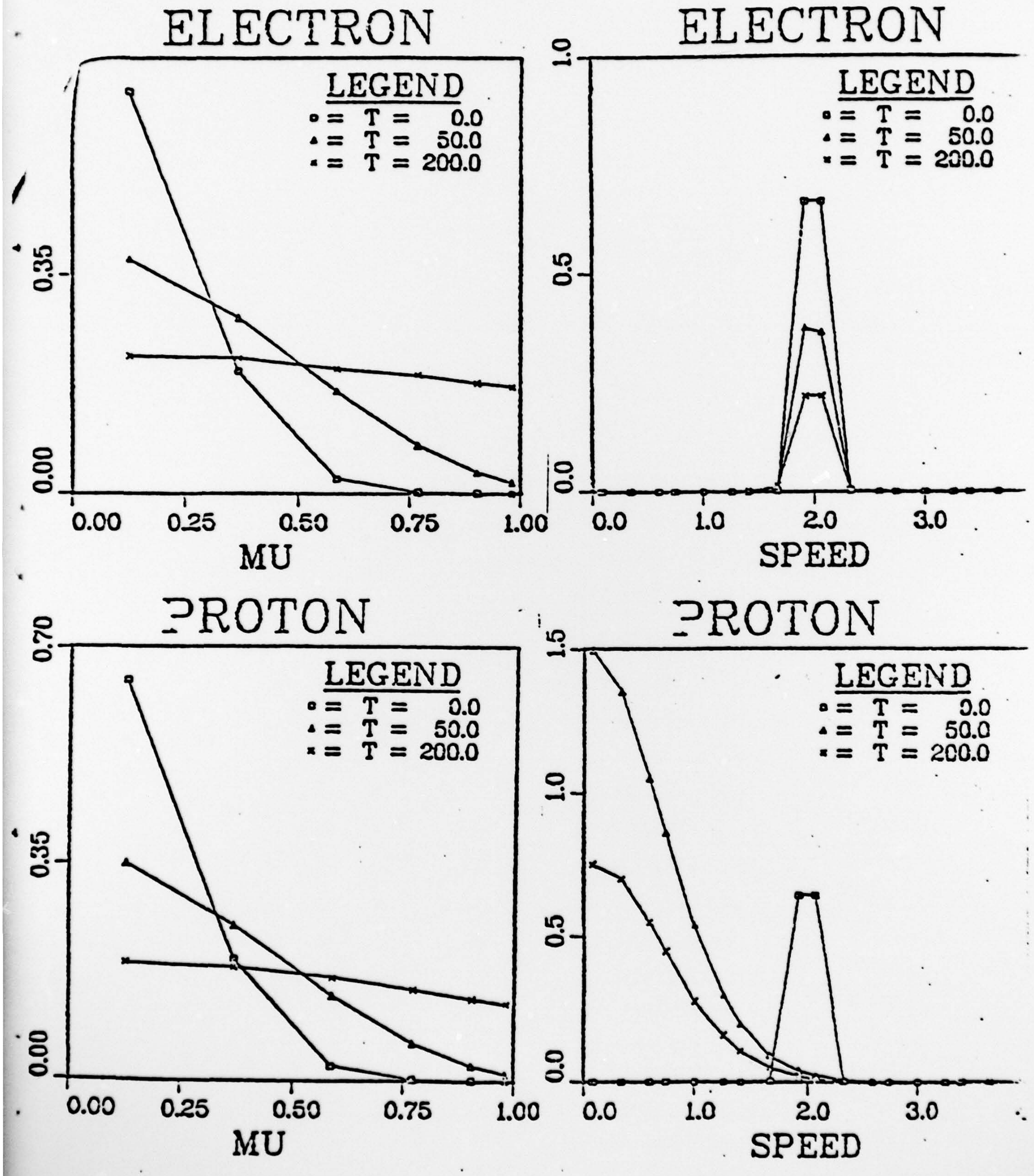
ELECTRON
LEGEND
▫ = T = 0.0
▴ = T = 50.0
× = T = 200.0
0.00
0.35
0.00
0.25
0.50
0.75
1.00
MU
ELECTRON
LEGEND
▫ = T = 0.0
▴ = T = 50.0
× = T = 200.0
1.0
0.5
0.0
0.0
1.0
2.0
3.0
SPEED
PROTON
LEGEND
▫ = T = 0.0
▴ = T = 50.0
× = T = 200.0
0.70
0.35
0.00
0.00
0.25
0.50
0.75
1.00
MU
PROTON
LEGEND
▫ = T = 0.0
▴ = T = 50.0
× = T = 200.0
1.5
1.0
0.5
0.0
0.0
1.0
2.0
3.0
SPEED

standard numerical approaches to radiation transport such as ray tracking and the variable Eddington method are quite useful for time-independent calculations, but become rather expensive when coupled to time-dependent hydrodynamic calculations.

Therefore much of our effort this past year has been directed at developing approximate radiation transport models more compatible with implementation in a fast-running hydrodynamics code. Two approaches have been studied thus far. The first is based on the frequency broadening of an emission line due to Doppler broadening during a series of absorptions and re-emissions. The second approach couples escape and transmission probability techniques for optically thin regions and diffusion (Eddington) theory for the optically thick regions.

The frequency broadening treatment has already been implemented in the hydrodynamics simulation code. The escape probability/diffusion model has been applied thus far only to a few regions modeled problems. The emission predictions of these two approaches will be compared to the results of a variable Eddington calculation to determine the validity of each model.

1. Frequency-Broadening Model

The basic idea inherent in this model is that the line profile widens to a width, x_1, where the optical depth, τ_1, equals one:

$$\tau_1 = 1 = \tau_o \exp(-x_1^2)$$

where τ_o is the optical depth at line center. The photons then escape from the wings of the line.

The time that it takes for a photon to escape is made up of two parts: the time for the radiation field to equilibrate (time for the profile to widen to x_1) and the escape time (time for the photon to escape after the field has equilibrated). The number of collisions (absorption/re-emission) that a photon makes before escaping can also be written as the sum of the number of collisions during each time interval. Once the number of collisions is known, the probability that a photon is quenched (photon energy removed from field in a non-radiative process) is given by

$$P = (1 - P_q)^{Q_s}$$

where P_q is the quenching probability per collision. The equilibration and escape times and the number of collisions are given by

$$t_1 = (\tau_o - 1)\, t_f \quad , \quad t_2 = 2\tau_o\, (\ln \tau_o)\, t_f \quad ,$$

$$Q_1 = \frac{\sqrt{\pi}}{2}\, (\ln \tau_o)^{-1} \quad , \quad Q_2 = \tau_o \sqrt{\pi \ln \tau_o} \quad , \quad Q_s = Q_1 + Q_2 \quad ,$$

and t_f is the mean time between collisions. Using the quenching probabilities, quenching rates are calculated for each region, and the resulting decrease in the radiation field is obtained. The net energy loss due to radiation is then used in the electron temperature calculation in the hydrodynamic simulation.

2. Escape Probability/Diffusion Model

If a zone is optically thin, first and second flight escape probabilities suffice to describe photon transport. The first flight escape probabilities for the central zone can be calculated in infinite, cylindrical geometry, while for the other regions, we can employ either cylindrical shell or slab geometries for calculating escape from the inner and outer surface areas. If all zones are thin, these probabilities alone are used to calculate total quenching and emission probabilities.

If a zone is optically thick, the diffusion equation with appropriate absorption and diffusion coefficients is solved using albedo boundary conditions. The absorption rate within the thick zone as well as emission at each surface is then calculated. Using these quantities and the escape and transmission probabilities of the surrounding thin zones, the total absorption and emission probabilities are calculated. These probabilities are presently being included in our MHD simulation models.

PAPERS PUBLISHED AND PRESENTED AT CONFERENCES

Ong, R.S.B. et al., "Collisional Effects on the Drift-Cyclotron Instability," Physica 83C, 237 (1976).

Kenney, D.J. and R.S.B. Ong, "Stimulated Brillouin Scattering in the Presence of a Magnetic Field," paper presented at the Sixth Annual Anomalous Absorption Conf., Vancouver, B.C. (1976).

Kenney, D.J., "Stimulated Brillouin Scattering in Magnetized Plasmas," Ph.D. Dissertation, Univ. of Michigan (1976).

Ionson, J.A. and R.S.B. Ong, "The Long Time Behavior of a Finite Amplitude Shear Alfven Wave in a Warm Plasma," Plasma Physics 18, 809 (1976).

Duston, D.P. and J.J. Duderstadt, "Radiation from Laser-Heated Metallic Exploding Wire Plasmas," paper presented at the APS Plasma Physics Division Annual Meeting, San Francisco, CA, Nov. 1976.

Ionson, J.A. and R.S.B. Ong, "Ion Acoustic Parametric Decay Instability in a Plasma with $\beta > 1$," Phys. Letters, 58A, 383 (1976).

Sheerin, J.P. and R.S.B. Ong, "On the Schrodinger Equation with Exponential Nonlinearity," paper presented at the Seventh Annual Symposium on Anomalous Absorption of Intense High-Frequency Waves, Ann Arbor, MI, May 1977.

Duston, D.P., "Theoretical Studies of the Radiation Hydrodynamics of Dense Laser-Heated Plasmas," Ph.D. Dissertation, Univ. of Michigan (1977).

Duderstadt, J.J. and D. Duston, "Ionization and Radiation Dynamics of Dense, MHD Plasmas," J. Appl. Phys. 49, 4388 (1978).

Duderstadt, J.J. and D. Duston, "X-ray Emission from Laser Heated Exploding Wires," Phys. Rev. A 18, 1707 (1978).

Duston, D.P. and J.J. Duderstadt, "Radiation from Laser-Heated Metallic Exploding Wire Plasmas," Bull. A.P.S. 21, 1039 (1978).

Ong, R.S.B. and A. Schmitt, "Thermal Self-Focusing of a Laser Beam in a Dense, Low Temperature Plasma," paper presented at the IEEE Int'l Conf. on Plasma Science, Montreal, Que., June 1979.

Duderstadt, J.J. and G. Moses, "PHD, A Plasma Hydrodynamics Code for Laser-Fusion Simulation Studies," Trans. Am. Nucl. Soc. 23, 50 (1976).

Duderstadt, J.J. and G. Moses, "Laser-Fusion Hydrodynamics Simulation," IEEE Symposium on Plasma Sciences (1976).

Melhorn, T. and J.J. Duderstadt, "Simulation of a Charged Particle Transport Using a Time-Dependent Fokker-Planck Code," Bull. A.P.S. 22 (1977).

Sheerin, J.P. and R.S.B. Ong, "On the Schrodinger Equation with Exponential Nonlinearity," Phys. Letters 63A, 279 (1977).

Melhorn, T. and J.J. Duderstadt, "Charged Particle Transport Using a Space and Time Dependent Fokker-Planck Code," paper presented at the IEEE Symposium on Plasma Science (1978).

Duderstadt, J.J. et al., "Characterization of an Ultra-Dense Reproducible Z-Pinch Plasma," App. Phys. Letter 31, 801 (1977).

Melhorn, T., "Charged Particle Transport Using a Space and Time Dependent Fokker-Planck Code," Ph.D. Dissertation, Univ. of Michigan (1978).

Ong, R.S.B. and J.P. Sheerin, "On Finite Amplitude Electrostatic Ion Cyclotron Wave," Bull. A.P.S. 23, 794 (1978).

Sheerin, J.P. and R.S.B. Ong, "Stability of Solitary Alfven Waves," Bull. A.P.S. 23, 816 (1978).

Sheerin, J.P. and R.S.B. Ong, "On the Stability of Solitary Kinetic Alfven Waves," accepted for publication in Phys. Letters (1979).

Duderstadt, J.J. and T.A. Melhorn, "A Discrete Ordinates Solution of the Fokker-Planck Equation Characterizing Charged Particle Transport," submitted for publication to J. Comp. Physics (1979).

REPORTS SUBMITTED DURING THE TENURE OF THE GRANT

J. Ionson and R.S.B. Ong, "The Long Time Behavior of a Finite Amplitude Shear Alfven Wave in a Warm Plasma," Technical Report, Oct. 1975.

J.J. Duderstadt, R.S.B. Ong, D.P. Duston, and D.J. Kenney, "Theoretical Studies of Laser Light Interaction and Optical and X-ray Emission from Dense Metallic Plasmas," Progress Report, Mar. 1976.

D.J. Kenney and R.S.B. Ong, "Stimulated Brillouin Scattering in Magnetized Plasmas," Technical Report, Aug. 1976.

J.J. Duderstadt, R.S.B. Ong, D.P. Duston, D.J. Kenney, and T. Melhorn, Annual Report I, Sept. 1976.

J.J. Duderstadt, R.S.B. Ong, D.P. Duston, T. Melhorn, and J. Sheerin, Progress Report II, May 1977.

D. Duston and J.J. Duderstadt, "X-ray Emission from Laser-Heated Exploding Wires," Technical Report, May 1977.

J.J. Duderstadt, R.S.B. Ong, D.P. Duston, T. Melhorn, and J.P. Sheerin, Annual Report II, Sept. 1977.

J.J. Duderstadt, R.S.B. Ong, D.P. Duston, T. Melhorn, and J.P. Sheerin, Annual Report III, Aug. 1978.

A. Schmitt and R.S.B. Ong, "Thermal Self-Focusing of a Laser Beam in a Dense Low Temperature Plasma," Technical Report, Feb. 1979.

J.P. Sheerin and R.S.B. Ong, "Solitary Alfven Wave-Guide Structures in a Magnetized Plasma," Technical Report, May 1979.